

A biological quarter-wave retarder with excellent achromaticity in the visible wavelength region

N. W. Roberts^{1,2*}, T.-H. Chiou³, N. J. Marshall³ and T. W. Cronin⁴

Animals make use of a wealth of optical physics to control and manipulate light, for example, in creating reflective animal colouration^{1–3} and polarized light signals⁴. Their precise optics often surpass equivalent man-made optical devices in both sophistication and efficiency⁵. Here, we report a biophysical mechanism that creates a natural full-visible-range achromatic quarter-wave retarder in the eye of a stomatopod crustacean. Analogous, man-made retardation devices are important optical components, used in both scientific research and commercial applications for controlling polarized light. Typical synthetic retarders are not achromatic, and more elaborate designs, such as, multilayer subwavelength gratings or bicrystalline constructions, only achieve partial wavelength independence⁶. In this work, we use both experimental measurements and theoretical modelling of the photoreceptor structure to illustrate how a novel interplay of intrinsic and form birefringence results in a natural achromatic optic that significantly outperforms current man-made optical devices.

The frequent discoveries in nature of biophotonic solids^{7,8}, novel scattering structures⁹ and complex diffractive architectures¹⁰ emphasize how the optical physics currently driving modern-day photonic technologies has already been used to great effect in living systems. In reality this is unsurprising, as the level of structural complexity and precision obtainable through natural self-assembly of biological materials far surpasses any current material manufacturing capabilities. This is particularly relevant to optical systems that work at ultraviolet (UV) and visible wavelengths, where the subwavelength scale of the architecture presents considerable technical challenges for manufacture.

Typically, optical structures in animals have evolved both for vision and for control of colouration. Colour is used for an array of tasks such as disruptive colouration and crypsis¹¹, as well as aposematic, aggressive and sexual signalling¹². However, for some animals, the control and detection of the polarization of light^{13,14} is equally important, particularly for animals whose photic environment renders colour signals untrustworthy as a source of information. One such group of animals is the stomatopod crustaceans. These marine animals have exceptionally sophisticated colour and polarization vision systems, with some species sensitive to both linearly and circularly polarized light^{15,16}. Their compound eyes contain a specialized midband with rows of aligned ommatidia, illustrated in Fig. 1a,b, and tiered photoreceptor cells. The species studied in this work, *Odontodactylus scyllarus*, was recently proven to discriminate between left and right handed circularly polarized light. It was proposed that a particular receptor type in the uppermost tier in 5th and 6th rows of the midband ommatidia enabled this discrimination by acting as an achromatic wave retarder¹⁶. This receptor is conventionally referred to as the 8th retinular

cell, or R8, and is known to display UV spectral sensitivity. Here, we reveal a novel biophysical mechanism responsible for achromatic retardation across the visible part of the spectrum.

In *O. scyllarus*, the photoreceptive regions, or rhabdomeres, of the R8 cells consist of a uniaxial microvillar assembly of lipid tubules containing photopigment^{14,17}. To begin to understand the optics of the achromatic retardation mechanism in the R8 cells, the inner and outer radii of the microvilli were first measured, and determined to be 26 and 40 nm, respectively (Fig. 1c). Clearly, these microvillar radii are subwavelength for visible light. The rhabdomeres of the R8 cells were measured to be 150 μm long. To then directly investigate the retardation properties of the R8 rhabdomeres, and the conversion between circularly and linearly polarized light, the S3 Stokes parameter was measured for incident light linearly polarized at 45° to the microvillar axis. Stokes parameters are a convenient mathematical way of describing the polarization of light. The four parameters (S0 to S3) can be used to describe both the ellipse of any arbitrary polarization and the degree of polarization, if the light contains an unpolarized component. If the magnitudes of the parameters are S0 = 1, S1 = 0, S2 = 0 and S3 = 1, then the light is right-hand circularly polarized. Figure 2 (points) details the magnitude of S3 for light transmitted through the R8 cell, showing the remarkable level of achromaticity in the majority of the visible wavelength range.

Achromatic retardation is an extremely unusual optical property, and greatly desirable in commercial devices¹⁸. The key to obtaining wavelength independence is correct dispersion in the birefringence of the system. This has been shown both theoretically and experimentally, for example, in the form birefringence of artificial subwavelength gratings (SWG)⁶. Form birefringence occurs in periodic structures with nanometric length scales, in which individual dielectric properties of constituent materials combine as effective values according to the boundary conditions of Maxwell's equations. In rhabdomeric photoreceptors, the scale of the microvilli and their periodic packing means that the dielectric properties of the microvilli and the cytoplasm combine as effective values to result in a form birefringent structure. Furthermore, the membranes of the microvilli are also intrinsically birefringent¹⁹, and the overall effective birefringence of the rhabdomere is given by the combination of both the intrinsic and form components.

We therefore hypothesized that interplay between the intrinsic and form birefringence explains the measured achromatic retardation in the R8 cell. To examine this, we adapted the general tensorial theory of periodic dielectrics set out by Bêche and Gaviot^{20,21} to derive the dielectric tensor for the R8 cell's rhabdomere as a function of wavelength. Using this to calculate the retardation in the cell, we then performed a grid search to minimize the S3 Stokes parameter to a value of unity. The anisotropic microvillar

¹Photon Science Institute, School of Physics and Astronomy, University of Manchester, Manchester M13 9PL, UK, ²School of Biological Sciences, University of Bristol, Woodland Road, Bristol BS8 1UG, UK, ³Sensory Neurobiology Group, School of Biomedical Sciences and Queensland Brain Institute, The University of Queensland, Brisbane, Queensland 4072, Australia, ⁴Department of Biological Sciences, University of Maryland Baltimore County, 1000 Hilltop Circle, Baltimore, Maryland 21250, USA. *e-mail: nicholas.roberts@bristol.ac.uk

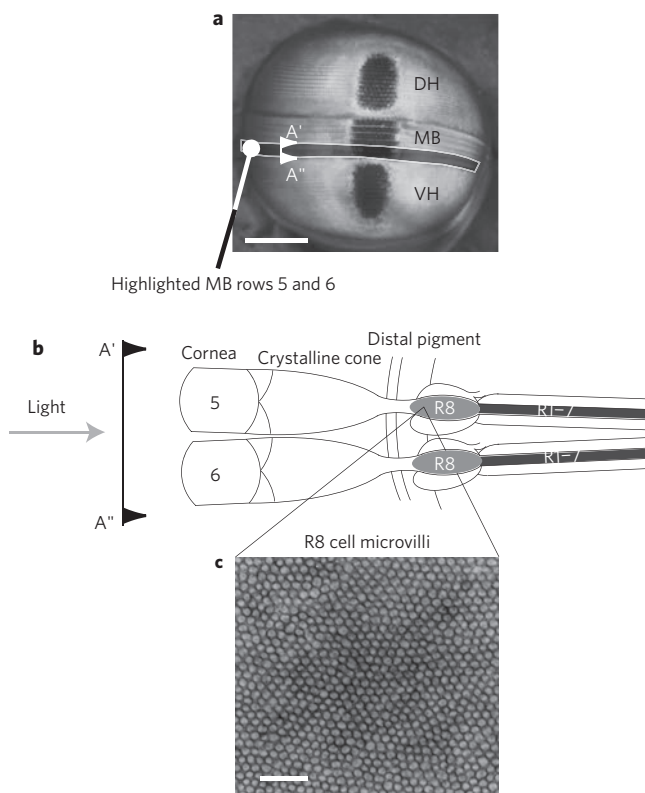


Figure 1 | The eye of a stomatopod crustacean. **a**, A frontal view of the compound eye of *Odontodactylus scyllarus* with the midband rows 5 and 6 highlighted by the greyed out region. VH, ventral hemisphere; DH, dorsal hemisphere; MB, midband. The section A'-A'' is shown schematically in **b**. This illustrates the arrangement of the 5th and 6th rows of the midband and the location of the 8th retinular cell (R8) quarter-wave retarder and the underlying R1-7 cells. The R8 cell is 150 μm long. **c**, Electron micrograph of the microvillar structure of the R8 cellular retarder. Scale bar, 200 nm.

cell membrane refractive indices and the associated dispersion were varied freely in the parameter space. A fixed parameter was the path length for the light and we used the microvilli radii measured above. We found that the R8 cell's long path length and low effective birefringence as a function of wavelength do indeed create a first-order achromatic quarter-wave retarder (Fig. 2, solid line). Importantly, the fitted values for the ideal intrinsic birefringence (Fig. 3a) are in excellent agreement with both the experimentally determined anisotropy in cell membranes, typically in the range 1.47–1.54 depending on the composition²² and functional form of the dispersion. The calculation also facilitates the examination of the dispersion in the effective refractive indices and birefringence of the R8 rhabdom (Fig. 3b). These results also agree closely with previous experimental measurements in invertebrate photoreceptors^{23,24}. Furthermore, the increase in the effective birefringence as a function of increasing wavelength clearly proves how the achromatic retardation is produced.

It is interesting to note that current man-made SWG retarders only achieve the same quality as the stomatopod's microvillar design over less than half this wavelength range. Figure 4 illustrates a comparison between the performance of the R8 cell and two man-made retardation devices. As would be expected, a quartz zero-order plate (dashed line) shows considerable variation across the visible wavelength range. A recent, highly efficient SWG structure²⁵, designed for operation at visible wavelengths (dotted line), shows a $\pm 9.1^\circ$ variation about the ideal quarter-wave retardation. In comparison, the R8 cell (solid line) only

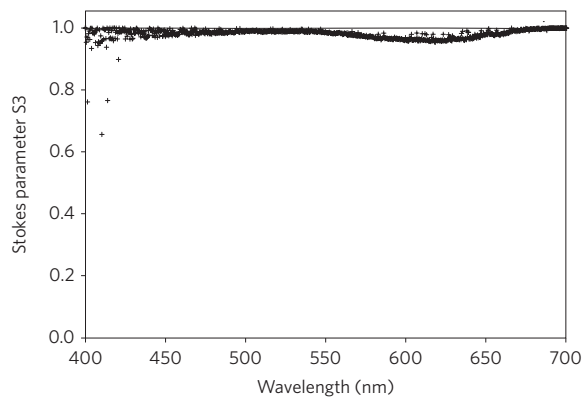


Figure 2 | Achromatic conversion of linearly to circularly polarized light by the R8 cell. Comparative experimental measurements (points) and calculated minimization (line) of the normalized Stokes parameter S3 for an ideal quarter-wave R8 retarder.

exhibits a $\pm 2.7^\circ$ variation, a performance better by a factor of three over the best man-made devices. A further novel property of this biological mechanism is the dependence of the retardation on the effective birefringence, optical path length and the absolute refractive index values. This is in direct contrast to typical commercial retarders.

The elegant nature of this biophysical mechanism emerges from the subwavelength optical architecture of the cellular structure. This complex and novel structural design exemplifies why natural photonic systems continue to offer biomimetic inspiration for the design and construction of new artificial photonic structures²⁶. In man-made optics, the required subwavelength periodicity presents significant challenges for manufacturing devices to operate at infrared and visible wavelengths (although recent metamaterials are approaching these length scales²⁷). In the biological optical system described here, natural selection has provided the solution to this construction problem. By selecting for specific geometric dimensions and optical properties within a cell type that has already evolved for efficient photoreception, relatively minor structural modifications have produced an excellent polarization control device. As Vukusic noted²⁸, animal systems commonly produce diverse optical properties by reorganizing the same biological materials.

Of further interest is the reason for the evolution of this degree of achromaticity. In the stomatopod eye, light transmitted through the R8 cells passes to an underlying larger photoreceptor element in which seven cells, all with a peak sensitivity near 511 nm, are fused together in a rhabdomeric column²⁹ (R1-7, Fig. 1b). This raises the question of why an achromatic quarter-wave retarder is favoured over one simply tuned to the photopigment's peak in these cells. The visual system needs to cope with the problem that the visual pigment absorbance spectra are broad, with typical half bandwidths (full-width at half-maximum, FWHM) close to 100 nm. This increases to more than 200 nm through self-screening in these very long receptor cells. An accurate broadband conversion of circularly to linearly polarized light by the R8 cell thus maximizes the polarization contrast for the differential analysis of circularly polarized light in this species.

In summary, we have discovered a novel microvillar mechanism that acts as a remarkable achromatic optical device. Man-made retarders are among the most important and commonly used optical components, and the cellular structure we describe significantly outperforms these current optics. This structure also offers potential biomimetic inspiration for a new category of optical devices, dual-purpose systems that would work as both microscopic spectral and polarization detectors and simultaneously as transmissive polarization control devices.

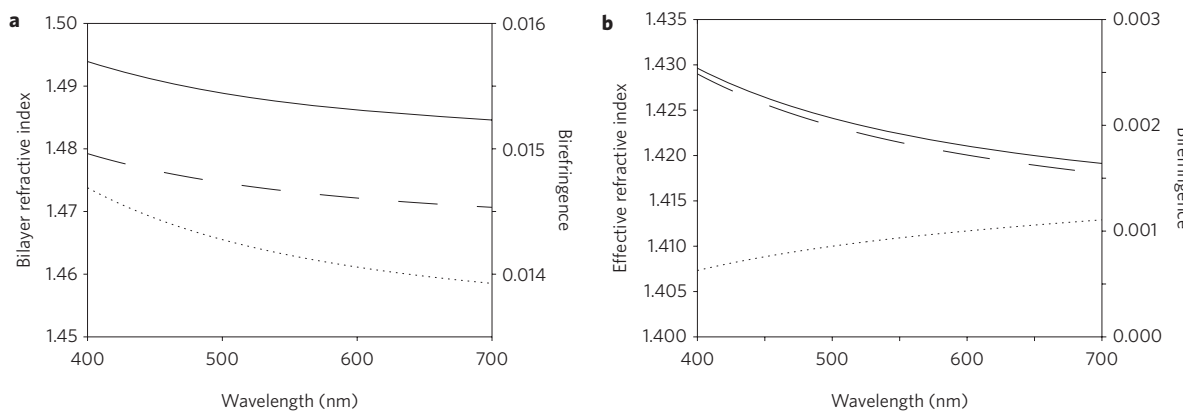


Figure 3 | Minimized refractive index and corresponding birefringence for the ideal *Odontodactylus scyllarus* R8 quarter-wave retarder in Fig. 2. a, The intrinsic refractive indices of the microvillar lipid membranes (solid and dashed lines) and the birefringence (dotted line). **b,** The effective refractive indices of the R8 rhabdom (solid and dashed lines) and the effective birefringence (dotted line).

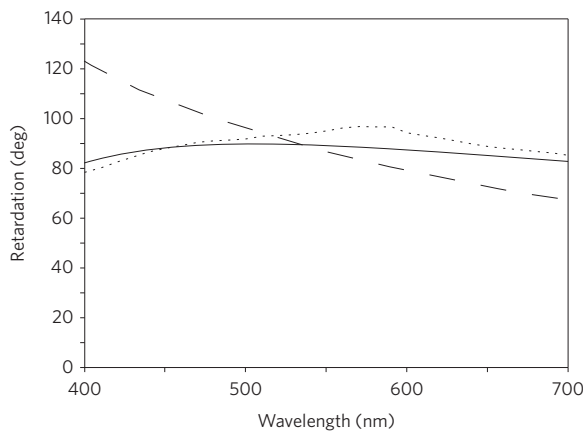


Figure 4 | Comparative retardation between two man-made quarter-wave retarders and the R8 cell. Both a quartz zero-order retarder (dashed line) and a subwavelength optimized grating²⁵ (dotted line) are significantly outperformed by the *Odontodactylus scyllarus* R8 cell mechanism (solid line).

Methods

Transmission electron microscopy (TEM). Eyes were fixed using a mixture of 4% glutaraldehyde and 0.5% paraformaldehyde in 0.1 M PIPES buffer with 2% sucrose and 1 mM EGTA (percentages by mass). Tissue was fixed at 4 °C overnight and post-fixation was carried out in 1% osmium tetroxide in PIPES buffer plus 2% sucrose, for 3 h. After dehydration in a series of ethanol, the material was passed through two changes of propylene oxide. It was rotated overnight in a mixture of 50% Spurr's resin and 50% propylene oxide, from which it was transferred into pure Spurr's resin and again rotated overnight before embedding. TEM was performed using thin sections cut using glass or diamond knives, stained with uranyl acetate and lead citrate, and examined on a Jeol 100C or a Zeiss EN 10CA TEM system.

Optical measurements. The experimental procedures in the optical Stokes parameter measurements have been described in detail previously¹⁶. Briefly, a polarizing microscope was used to measure the Stokes parameters of the transmitted light through 10-μm transverse cryosections of the R8 cell rhabdomeres from the 5th and 6th midband rows from *O. scyllarus*. The optical properties of the individual sections were converted to the full measured path length of the photoreceptor cell. This was determined by counting the number of sections that comprised the cell's full length.

Optical modelling. The calculation methods for three-dimensional photoreceptor dielectric tensors have also been described in detail previously²² and use the formalism set out by Béche and Gaviot²⁰. For this work, the modelling was extended through a grid search to minimize the anisotropic dispersion parameters in the membrane bilayers, as defined by the Sellmeier equation³⁰. The topography of the four-dimensional parameter space used in the search was monitored throughout the minimization to ensure that the global minimum was obtained.

Received 28 July 2009; accepted 25 September 2009; published online 25 October 2009

References

- Vukusic, P. & Hooper, I. Directionally controlled fluorescence emission in butterflies. *Science* **310**, 1151 (2005).
- Vukusic, P., Sambles, J. R. & Lawrence, C. R. Structural colour—colour mixing in wing scales of a butterfly. *Nature* **404**, 457 (2000).
- Sutherland, R. L., Mathger, L. M., Hanlon, R. T., Urbas, A. M. & Stone, M. O. Cephalopod coloration model. I. Squid chromatophores and iridophores. *J. Opt. Soc. Am. A* **25**, 588–599 (2008).
- Cronin, T. W. *et al.* Polarization vision and its role in biological signaling. *Integr. Comparat. Biol.* **43**, 549–558 (2003).
- Vukusic, P. & Sambles, J. R. Photonic structures in biology. *Nature* **424**, 852–855 (2003).
- Kikuta, H., Ohira, Y. & Iwata, K. Achromatic quarter-wave plates using the dispersion of form birefringence. *Appl. Opt.* **36**, 1566–1572 (1997).
- Morris, R. B. Iridescence from diffraction structures in the wing scales of *Callophrys rubi*, the green hairstreak. *J. Entomol. A* **49**, 149–154 (1975).
- Parker, A. R., Welch, V. L., Driver, D. & Martini, N. Structural colour—opal analogue discovered in a weevil. *Nature* **426**, 786–787 (2003).
- Vigneron, J. P. *et al.* Switchable reflector in the Panamanian tortoise beetle *Charidotella egregia* (Chrysomelidae:Cassidinae). *Phys. Rev. E* **76**, 031907 (2007).
- Vukusic, P., Sambles, J. R., Lawrence, C.R. & Wotton R. J. Structural colour—now you see it now you don't. *Nature* **410**, 36 (2001).
- Cuthill, I. C. *et al.* Disruptive coloration and background pattern matching. *Nature* **434**, 72–74 (2005).
- Endler, J. A. On the measurement and classification of color in studies of animal color patterns. *Biol. J. Linn. Soc.* **41**, 315–352 (1990).
- Roberts, N. W. & Needham, M. G. A mechanism of polarized light sensitivity in cone photoreceptors of the goldfish *Carassius auratus*. *Biophys. J.* **93**, 3241–3248 (2007).
- Marshall, N. J. *et al.* The compound eyes of mantis shrimps (Crustacea, Hoplocarida, Stomatopoda). 1. Compound eye structure—the detection of polarized light. *Philos. Trans. Roy. Soc. B* **334**, 33–56 (1991).
- Marshall, N. J., Cronin, T. W., Shashar, N. & Land, M. Behavioural evidence for polarisation vision in stomatopods reveals a potential channel for communication. *Curr. Biol.* **9**, 755–758 (1999).
- Chiou, T.-H. *et al.* Circular polarization vision in a stomatopod crustacean. *Curr. Biol.* **18**, 429–434 (2008).
- Marshall, N. J. *et al.* The compound eyes of mantis shrimps (Crustacea, Hoplocarida, Stomatopoda). 2. Color pigments in the eyes of stomatopod crustaceans—polychromatic vision by serial and lateral filtering. *Philos. Trans. Roy. Soc. B* **334**, 57–84 (1991).
- Tilsch, M. K. *et al.* Production scale deposition of multilayer film structures for birefringent optical components. *Thin Solid Films* **516**, 107–113 (2007).
- Kirschfeld, K. & Snyder, A. W. *Photoreceptor Optics* 56–77 (Springer, 1975).
- Béche, B. & Gaviot, E. Matrix formalism to enhance the concept of effective dielectric constant. *Opt. Commun.* **219**, 15–19 (2003).
- Roberts, N. W. & Gleeson, H. F. The absorption of polarized light by vertebrate photoreceptors. *Vision Res.* **44**, 2643–2652 (2004).
- Roberts, N. W. The optics of vertebrate photoreceptors: anisotropy and form birefringence. *Vision Res.* **46**, 3259–3266 (2006).

23. Wehner, R., Bernard, G. D. & Geiger, E. Twisted and non-twisted rhabdoms and their significance for polarization detection in the bee. *J. Comp. Physiol.* **104**, 225–245 (1975).
24. Snyder, A. W. & McIntyre, P. *Photoreceptor Optics* 338–391 (Springer, 1975).
25. Yi, D. E., Yan, Y. B., Liu, H. T., Si-Lu & Jin, G. F. Broadband achromatic phase retarder by subwavelength grating. *Opt. Commun.* **227**, 49–55 (2003).
26. Gaillot, D. P. *et al.* Composite organic–inorganic butterfly scales: production of photonic structures with atomic layer deposition. *Phys. Rev. E* **78**, 031922 (2008).
27. Valentine, J. *et al.* Three-dimensional optical metamaterial with a negative refractive index. *Nature* **455**, 376–379 (2008).
28. Vukusic, P., Hallam, B. & Noyes, J. Brilliant whiteness in ultrathin beetle scales. *Science* **315**, 348 (2007).
29. Cronin, T. W., Marshall, N. J. & Caldwell, R. L. Visual pigment diversity in two genera of mantis shrimps implies rapid evolution (Crustacea; Stomatopoda). *J. Comp. Physiol. A* **179**, 371–384 (1996).
30. Jenkins, F. A. & White, H. E. *Fundamentals of Optics* 4th edn, 482 (McGraw-Hill International Editions, 1981).

Acknowledgements

This work was supported by grants from the Air Force Office of Scientific Research, the Engineering and Physical Sciences Research Council (EPSRC), the Asian Office of Aerospace Research and Development, the Australian Research Council and the National Science Foundation.

Author contributions

All authors contributed extensively to all aspects of the work presented in this paper.

Additional information

Reprints and permission information is available online at <http://npg.nature.com/reprintsandpermissions/>. Correspondence and requests for materials should be addressed to N.W.R.